

A new type of charged defect in amorphous chalcogenides.

S. I. Simdyankin,^{1,*} T. A. Niehaus,² G. Natarajan,¹ Th. Frauenheim,² and S. R. Elliott¹

¹*Department of Chemistry, University of Cambridge,
Lensfield Road, Cambridge CB2 1EW, United Kingdom*

²*Fachbereich 6 — Theoretische Physik, Universität Paderborn,
Warburger Straße 100, D-33098, Paderborn, Germany*

(Dated: June 15, 2021)

We report on density-functional-based tight-binding (DFTB) simulations of a series of amorphous arsenic sulfide models. In addition to the charged coordination defects previously proposed to exist in chalcogenide glasses, a novel defect pair, $[\text{As}_4]^- - [\text{S}_3]^+$, consisting of a four-fold coordinated arsenic site in a seesaw configuration and a three-fold coordinated sulfur site in a planar trigonal configuration, was found in several models. The valence-alternation pairs $[\text{S}_3]^+ - \text{S}_1^-$ are converted into $[\text{As}_4]^- - [\text{S}_3]^+$ pairs under HOMO-to-LUMO electronic excitation. This structural transformation is accompanied by a decrease in the size of the HOMO-LUMO band gap, which suggests that such transformations could contribute to photo-darkening in these materials.

PACS numbers: 71.23.Cq, 61.43.Dq,

Amorphous chalcogenides, i.e. sulfides, selenides and tellurides, are distinguished from other materials by their photosensitivity. These materials exhibit intriguing photo-induced phenomena that are not observed in their crystalline counterparts. Some of these unusual phenomena have many potential applications [1]. A detailed microscopic understanding of the origin of these phenomena [2], however, is still lacking.

In the context of photo-induced structural changes, special significance is attributed to the presence of oppositely charged coordination-defect (valence-alternation) pairs [3]. Normally, such defect pairs contain singly-coordinated chalcogen atoms having distinct spectroscopic signatures [3]. Experimentally, the concentration of these defects is estimated to be rather small [4], i.e. 10^{17} cm^{-3} , compared with the atomic density of about $2 \times 10^{25} \text{ cm}^{-3}$, in order quantitatively to account for the observed magnitude of the photo-induced effects.

Here, we investigate the structure of, and simulate photo-structural changes in, a series of computer-generated models of the archetypal amorphous chalcogenide, diarsenic trisulfide (a- As_2S_3). In addition to the well-known [3] valence-alternation pairs (VAPs) $[\text{C}_3]^+ - \text{C}_1^-$ and $\text{P}_4^+ - \text{C}_1^-$, where C_n/P_n stands for an n -fold coordinated chalcogen/pnictogen (e.g. sulfur/arsenic) atom, some of the models were found to contain the previously unreported $[\text{P}_4]^- - [\text{C}_3]^+$ defect pairs. These defect pairs are unusual in two ways. First, there is an excess of *negative* charge in the vicinity of the normally electropositive pnictogen atoms and, second, there are no under-coordinated atoms with dangling bonds in these local configurations. The latter peculiarity may be the reason why such defect pairs have not yet been identified experimentally.

All our simulations have been done by using a density-functional-based tight-binding method [5], unless specified otherwise. We found that a basis set of s, p and d

Slater-type orbitals for all atoms is an essential prerequisite for the observation of the defect-related effects reported here [6]. Each of our models contained 60 (24 As and 36 S) atoms. This size of model was chosen so as to be big enough that the defect pairs could be accommodated within the volume of the periodic simulation box, and yet small enough to allow for the creation and analysis of several statistically independent models in a reasonable time. The quality of the models, in terms of comparison with experimental neutron-diffraction data, is similar to that of the larger models reported in Ref. 7.

By using NVT (constant number of particles, volume, and temperature) molecular-dynamics simulations, we first created a 24-atom model of amorphous arsenic by quenching from the melt. Three-fold coordination was imposed by iteratively modifying the nearest-neighbor shell of each atom and bringing the system to thermal equilibrium at room temperature. A stoichiometric model (model 0, in the following) of a- As_2S_3 was then created by decorating each of the As-As bonds with S atoms, followed by rescaling the model to the experimental density [8] $\rho = 3.186 \text{ g/cm}^3$ and relaxing at room temperature ($T = 300 \text{ K}$). This model was then melted at $T = 3000 \text{ K}$ and ten more models were created by taking snapshots of the 3000 K molecular-dynamics trajectory at irregular time intervals as starting configurations, and following the cooling schedule described in Ref. 7.

The defect statistics for the models containing coordination defects are shown in Table I. The coordination numbers were calculated as the number of nearest neighbors within a spherical shell of a radius corresponding to the position of the first minimum in the corresponding partial radial distribution function. The numbers in each triplet in Table I show, respectively, the number of corresponding defects in (I) the as-prepared ground-state optimized geometry, (II) the excited-state geometry optimized under the constraint of having one electron in

TABLE I: Defect statistics for the models containing coordination defects. Each triplet of numbers denotes, respectively, (I) the number of defects in the as-prepared ground state, (II) HOMO-LUMO-promoted excited state, and (III) the ground state resulting from the excited state.

Model	Number of					
	coordination defects				homopolar bonds	
	As ₂	As ₄	S ₁	S ₃	As-As	S-S
0	0,1,0	0,0,0	0,1,0	0,0,0	0,0,0	0,0,0
1	0,1,0	1,1,1	0,0,0	1,0,1	1,1,1	1,1,1
2	0,2,0	0,0,1	1,0,0	1,0,1	2,1,2	2,2,2
3	0,0,0	1,1,1	1,1,1	0,0,0	1,1,1	0,0,0
5	0,0,0	0,0,0	0,1,0	0,0,0	1,1,1	1,0,1
6	0,0,0	1,0,1	0,1,0	1,1,1	2,2,2	2,2,2
10	0,1,0	0,0,1	1,0,0	1,1,1	1,0,1	1,1,1

the highest occupied molecular orbital (HOMO) and one electron in the lowest unoccupied orbital (LUMO), and (III) the ground-state optimized geometry obtained from the excited-state configuration. Although electronic excitations where one electron is promoted from HOMO to LUMO Kohn-Sham states [9] are not especially realistic, we simulate such excitations in order qualitatively to assess defect stability with respect to (optically-induced) electronic excitations. Note that in models 2 and 10, S₃-S₁ defect pairs converted into As₄-S₃ pairs as a result of the electronic excitation.

The statistics of Mulliken charges (in atomic units) were calculated for all 11 models in the ground state before and after electronic excitation. Since all extremal charge values, which significantly deviate from the average values (0.32 for As, -0.21 for S), correspond to coordination defects, these data confirm that the coordination defects form charged defect pairs. The maximum positive charge (0.46) is on a four-fold coordinated As atom that is part of an intimate valence-alternation pair (IVAP) where a singly coordinated S atom is covalently bonded to it. The minimum positive charge (0.07) is on an As atom that forms a homopolar bond with an As₄ center (see Table II). The minimum negative charge (-0.36) is on a singly coordinated S atom, and the maximum negative charge (-0.03) is on a S atom that forms a homopolar bond with another S atom with a similar charge value.

It is common [3] to use the following notation for valence-alternation pairs: As₄⁺-S₁⁻ and S₃⁺-S₁⁻, where the superscripts show the polarity of the nominal excess charge on corresponding defect centers. Although the charges on As₄ and S₁ atoms are of correct polarity in an alloy of normally electropositive As and electronegative S, those on S₃ are not. Therefore, it is more appropriate to use the notation [S₃]⁺ for three-fold coordinated S atoms, where the square brackets imply that the excess charge is distributed between the center and its nearest neighbors. Table II shows that there is also an excess

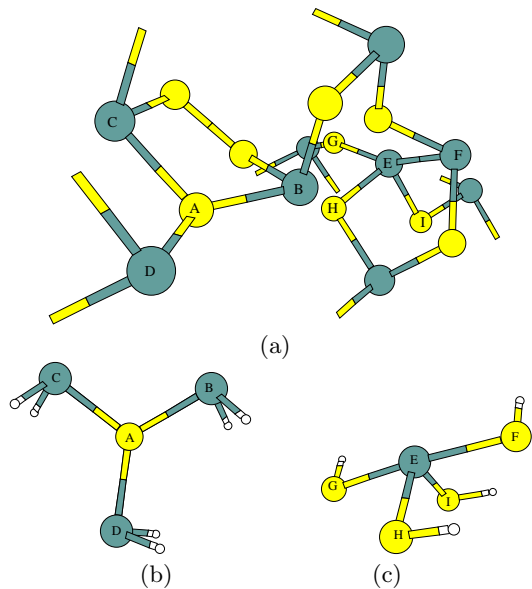


FIG. 1: Planar trigonal, [S₃]⁺ (marked by letter ‘A’), and seesaw, [As₄]⁻ (marked by letter ‘E’), configurations in (a) a fragment of model 2(III) (the dangling bonds show where the displayed configuration connects to the rest (not shown) of the network) and, (b) and (c), charged isolated clusters (the dangling bonds are terminated with hydrogen atoms). The shading of the As atoms is darker than that of the S atoms. Bond lengths are (Å): (a) AB=AD=2.42, AC=2.39, EF=2.83, EG=2.54, EH=2.35, EI=2.33; (b) AB=2.34, AC=AD=2.33; (c) EF=2.55, EG=2.46, EH=2.30, EI=2.32. Color online.

negative charge in the vicinity of As₄ centers when [S₃]⁺ centers are also present, and these newly-identified defects will be denoted as [As₄]⁻ here.

It is of interest to verify whether the excess charge has a similar effect on the local structure in both super-cell amorphous and isolated cluster models. Fig. 1(a) shows a fragment of model 2(III) containing both [As₄]⁻ and [S₃]⁺ defects. Fig. 1 also shows the optimized geometry in (b) [SAs₃H₆]⁺ and (c) [AsS₄H₄]⁻ clusters, where one electron was removed from and added to the neutral system, respectively. The seesaw [As₄]⁻ and planar [S₃]⁺ local configurations observed in models 1(I), 2(III) (see Fig. 1(a)), 6(I) and 10(III) are indeed very similar to those in the isolated clusters shown in Fig. 1 (b) and (c), respectively. We note that similar seesaw-like structures are also observed in local configurations around hypervalent chalcogens, e.g. in sulfur(IV) fluoride and in certain tellurides [10], and are expected from stereochemical considerations [11]. Also, the five-fold coordinated As defect reported in [12] can be viewed as an [As₄]⁻ center bonded to an additional As atom (placed on top of the structure depicted in Fig. 1(c)). Interestingly, five-membered rings fit conveniently to parts of the over-coordinated defect centers, which might contribute to the stability of this type of defect pair. It is also worth mentioning that there is a distinct pattern in the distribution of charges

TABLE II: Mulliken charges, in atomic units, on atoms within the $[\text{As}_4]^- - [\text{S}_3]^+$ defect pairs. The index (I) next to the model number signifies the as-prepared ground-state geometry, and (III) indicates the ground-state structure obtained by geometry optimization of the excited-state configuration (II). The relevant fragment of model 2(III) and clusters $[\text{SAs}_3\text{H}_6]^+$ and $[\text{AsS}_4\text{H}_4]^-$ are depicted in Fig. 1(a)-(c), respectively.

Model	Center	Neighbors				Total
		1	2	3	4	
1(I)	(As) 0.313	(S) -0.194	(S) -0.281	(S) -0.223	(S) -0.313	-0.698
	(S) -0.110	(As) 0.363	(As) 0.379	(As) 0.362		0.994
2(III)	(As) 0.329	(As) 0.071	(S) -0.221	(S) -0.203	(S) -0.329	-0.353
	(S) -0.153	(As) 0.355	(As) 0.347	(As) 0.351		0.900
6(I)	(As) 0.345	(S) -0.149	(S) -0.255	(S) -0.295	(S) -0.225	-0.579
	(S) -0.146	(As) 0.375	(As) 0.376	(As) 0.384		0.989
10(III)	(As) 0.326	(As) 0.101	(S) -0.242	(S) -0.308	(S) -0.231	-0.354
	(S) -0.158	(As) 0.363	(As) 0.295	(As) 0.101		0.601
$[\text{AsS}_4\text{H}_4]^-$	(As) 0.280	(S) -0.359	(S) -0.320	(S) -0.498	(S) -0.600	-1.497
$[\text{SAs}_3\text{H}_6]^+$	(S) -0.149	(As) 0.365	(As) 0.362	(As) 0.374		0.952

in the seesaw configuration, which is most clearly seen in the isolated $[\text{AsS}_4\text{H}_4]^-$ cluster, — the more distant sulfur atoms F and G (see Fig. 1(c)) have the largest magnitude negative charges (see Table II).

Although the DFTB method involves a number of approximations, it has been shown [5] that its accuracy is comparable to that of full DFT methods. In order to verify whether the $[\text{As}_4]^- - [\text{S}_3]^+$ defect pair is reproducible with more accurate methods, we optimized the geometry of model 1(I) by SIESTA [13], which is a DFT method using an atomic-orbital basis set and pseudopotentials to eliminate the core electrons. Apart from insignificant changes in bond lengths and angles, the SIESTA- and DFTB-optimized models are very similar, including the region with the seesaw-planar trigonal defect pair. We also performed high-accuracy all-electron geometry optimization of the isolated charged clusters shown in Fig. 1(b) and (c) by using NWChem [14, 15]. The calculations were performed at the all-electron DFT level with a B3LYP hybrid exchange-correlation functional and a 6-311G** gaussian basis set which includes s, p and d orbitals on the sulfur and arsenic atoms. The optimized DFTB geometry was used as a starting configuration for the all-electron optimizations. After optimization, the shapes of the molecular clusters were preserved, apart from a slight increase in the bond lengths, EF=2.80 Å and EG=2.51 Å, in the “seesaw” configuration.

We have found that the hitherto unreported $[\text{As}_4]^- - [\text{S}_3]^+$ defect pairs in our models are stable with respect to HOMO-to-LUMO electron excitations. We also performed a geometry optimization of an $\text{As}_4\text{S}_{10}\text{H}_8$ cluster, containing an $[\text{As}_4]^- - [\text{S}_3]^+$ pair by construction, both in the ground state and in the first singlet excited state within the linear-response approximation to time-dependent density-functional theory, which gives a much better description of excited states compared with

HOMO-to-LUMO electron excitations [16] (see Fig. 2). Although the bond AC in the ground-state structure depicted in Fig. 2(a) is significantly elongated, analysis of the electron density in the HOMO and LUMO electronic states (see Fig. 2(b)) shows that it has a significant bonding character, implying that this cluster contains a distorted $[\text{As}_4]^- - [\text{S}_3]^+$ pair. As seen in Fig. 2(c), redistribution of the electron density in the excited state leads to a symmetrization of the As_4 center and to an elongation of the bond BE in the region of the S_3 center, where the LUMO electronic state is predominantly localized. Subsequent geometry optimization of the excited-state configuration results in the same ground-state geometry as in Fig. 2(a). We observed that bond breaking/elongation in all our models generally occurs at the groups of atoms where the LUMO is localized, indicating the expected antibonding character of LUMO states.

The HOMO-LUMO band-gap energies for models 0-10 are listed in Table III. As in Table I, the three values correspond, respectively, to the same ground-, excited-, ground-state geometries. Note that in models 2 and 10, the magnitude of the band gap has decreased as $[\text{S}_3]^+ - \text{S}_1^-$ pairs were converted into $[\text{As}_4]^- - [\text{S}_3]^+$ pairs. It should be noted that $[\text{S}_3]^+$ centers are not necessarily conserved under such conversions — while in model 10 the S_3 atom is the same in both ground states (I) and (III), in model 2 it is not.

In summary, we have demonstrated the existence of a new type of charged defect pair in amorphous arsenic sulfide, namely $[\text{As}_4]^- - [\text{S}_3]^+$, where the As center has a “seesaw” configuration, and the S center is trigonal planar. A plausible scenario for photo-darkening in this material is the conversion of other types of defects containing under-coordinated atoms into such defect pairs due to electronic excitation under illumination. Interestingly, in the two models where such conversion has been observed, As-As

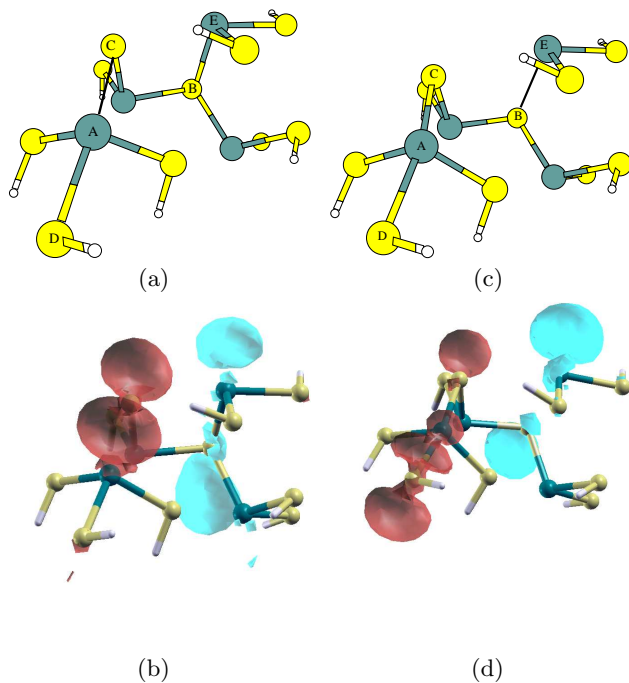


FIG. 2: An $\text{As}_4\text{S}_{10}\text{H}_8$ cluster containing both defect centers $[\text{As}_4]^-$ (marked by letter ‘A’) and $[\text{S}_3]^+$ (‘B’). The shading of the atoms is the same as in Fig 1. The black solid lines signify elongated bonds. (a) Optimized ground-state geometry. Bond lengths are (\AA): $\text{AC}=3.00$, $\text{AD}=2.32$, and $\text{BE}=2.4$. (b) Isosurfaces corresponding to the value of 0.025 of electron density in the HOMO (darker red surface) and LUMO (lighter cyan surface) states for the structure shown in (a). (c) Optimized geometry in the first singlet excited state. Bond lengths are (\AA): $\text{AC} = 2.43$, $\text{AD} = 2.44$, and $\text{BE} = 2.82$. (d) Same as (b), but for the structure shown in (c). Color online.

TABLE III: HOMO-LUMO band-gap energies for the all-heteropolar model 0 and the models containing coordination defects. The indices (I), (II), (III) correspond to the triplets in Table I.

Model	Band gap (eV)		
	(I)	(II)	(III)
0	1.46	0.68	1.46
1	1.13	0.94	1.13
2	1.41	0.62	1.06
3	1.23	0.21	1.24
4	1.47	1.50	1.47
5	1.68	0.40	1.67
6	1.47	1.37	1.47
7	1.47	1.50	1.47
8	1.38	1.20	1.38
9	1.65	1.31	1.65
10	1.20	0.85	1.02

homopolar bonds were formed as part of the $[\text{As}_4]^-$ centers. Given that their bond lengths are greater than the average bond length in the material, such bond formation could also contribute to photo-expansion of the material.

S.I.S. and G.N. are grateful to the EPSRC for financial support. We thank the British Council and DAAD for provision of financial support. We used the XMakeMol [17] and XCrySDen [18] software for visualization.

* Electronic address: sis24@cam.ac.uk

- [1] H. S. Nalwa, ed., *Handbook of Advanced Electronic and Photonic Materials and Devices*, vol. 5: Chalcogenide Glasses and Sol-Gel Materials (Academic Press, San Diego, 2001).
- [2] A. V. Kolobov, ed., *Photo-Induced Metastability in Amorphous Semiconductors* (Wiley-VCH, Weinheim, 2003).
- [3] M. Kastner, D. Adler, and H. Fritzsche, *Phys. Rev. Lett.* **37**, 1504 (1976).
- [4] A. Feltz, *Amorphous Inorganic Materials and Glasses* (VCH, Weinheim, 1993), p. 203.
- [5] T. Frauenheim, G. Seifert, M. Elstner, T. Niehaus, C. Köhler, M. Amkreutz, M. Sternberg, Z. Hajnal, A. D. Carlo, and S. Suhai, *J. Phys.: Condens. Matter* **14**, 3015 (2002).
- [6] S. I. Simdyankin, S. R. Elliott, T. A. Niehaus, and T. Frauenheim, in *Proceedings of 3rd International Conference “Computational Modeling and Simulation of Materials”* (Techna Group s.r.l., Faenza, Italy, 2004), in press.
- [7] S. I. Simdyankin, S. R. Elliott, Z. Hajnal, T. A. Niehaus, and T. Frauenheim, *Phys. Rev. B* **69**, 144202 (2004).
- [8] J. H. Lee, A. C. Hannon, and S. R. Elliott, *Neutron scattering studies of arsenic sulphide glasses*, eprint: cond-mat/0402587.
- [9] X. Zhang and D. A. Drabold, *Phys. Rev. Lett.* **83**, 5042 (1999).
- [10] J. C. McLaughlin, S. L. Tagg, J. W. Zwanziger, D. R. Haefner, and S. D. Shastri, *J. Non-Cryst. Solids* **274**, 1 (2000).
- [11] M. North, *Principles and Applications of Stereochemistry* (Stanley Thornes, Cheltenham, 1998).
- [12] T. Uchino, D. C. Clary, and S. R. Elliott, *Phys. Rev. Lett.* **85**, 3305 (2000).
- [13] J. M. Soler, E. Artacho, J. D. Gale, A. García, J. Junquera, P. Ordejón, and D. Sánchez-Portal, *J. Phys. Condens. Matter* **14**, 2745 (2002).
- [14] R. A. Kendall, E. Aprá., D. Bernholdt, E. J. Bylaska, M. Dupuis, G. I. Fann, R. J. Harrison, J. Ju, J. Nichols, J. Nieplocha, et al., *Computer Phys. Comm.* **128**, 260 (2000).
- [15] Straatsma, T.P.; Aprá, E.; Windus, T.L.; Bylaska, E.J.; de Jong, W.; Hirata, S.; Valiev, M.; Hackler, M. T.; Pollack, L.; Harrison, R. J.; Dupuis, M.; Smith, D.M.A.; Nieplocha, J.; Tipparaju V.; Krishnan, M.; Auer, A. A.; Brown, E.; Cisneros, G.; Fann, G. I.; Fruchtl, H.; Garza, J.; Hirao, K.; Kendall, R.; Nichols, J.; Tsemekhman, K.; Wolinski, K.; Anchell, J.; Bernholdt, D.; Borowski, P.; Clark, T.; Clerc, D.; Dachsels, H.; Deegan, M.; Dyall,

- K.; Elwood, D.; Glendening, E.; Gutowski, M.; Hess, A.; Jaffe, J.; Johnson, B.; Ju, J.; Kobayashi, R.; Kutteh, R.; Lin, Z.; Littlefield, R.; Long, X.; Meng, B.; Nakajima, T.; Niu, S.; Rosing, M.; Sandrone, G.; Stave, M.; Taylor, H.; Thomas, G.; van Lenthe, J.; Wong, A.; Zhang, Z.; "NWChem, A Computational Chemistry Package for Parallel Computers, Version 4.6" (2004), Pacific Northwest National Laboratory, Richland, Washington 99352-0999, USA.
- [16] T. A. Niehaus, S. Suhai, F. D. Sala, P. Lugli, M. Elstner, G. Seifert, and T. Frauenheim, *Phys. Rev. B* **63**, 085108 (2001).
- [17] M. P. Hodges, *Xmakemol homepage*, URL <http://www.nongnu.org/xmakemol/>.
- [18] A. Kokalj, *J. Mol. Graphics Modelling* **17**, 176 (1999), URL <http://www.xcrysden.org/>.